ACI STRUCTURAL JOURNAL TECHNICAL PAPER

Title no. 106-S12

Experimental Analysis on Tensile Dynamic Behavior of Existing Concrete under High Strain Rates

by Domenico Asprone, Ezio Cadoni, and Andrea Prota

The presented research is part of a wider research project involving the study of the dynamic behavior under extreme loads of the Tenza Bridge, a concrete arch bridge located in southern Italy. The dynamic behavior of the concrete of the bridge under tensile loads is herein investigated. Several dynamic tensile tests under different strain rates were performed on concrete specimens at the DynaMat laboratory of the University of Applied Sciences of Southern Switzerland using modified Hopkinson bars. The results were then processed in terms of strength dynamic increase factor-strain rate relationships. These are fundamental to assess constitutive laws of concrete to be implemented in analytical models of the bridge under dynamic loads. The results are compared with existing analytical formulations that attempt to predict the dynamic tensile strength of concrete. The comparisons show that, even though tested concrete was taken from an existing structure, the relationships found in the literature accurately describe its tensile dynamic behavior.

Keywords: dynamic behavior; loads; strain; tensile strength.

INTRODUCTION

Nowadays, structural design of some critical infrastructures has to allow for events such as blasts, impacts, or strong earthquakes, which force such structures to withstand severe dynamic load conditions, characterized by high intensity and short duration. Therefore, dynamic properties of materials play a fundamental role in the evaluation of the structural behavior of critical infrastructures under such particular events. The activities presented in the current paper, part of a wider research project—namely, the Tenza project—are related to this topic.

The objective of the Tenza project is to study the effect of high dynamic loads on a reinforced concrete (RC) arch bridge that is part of the abandoned path of the Salerno-Reggio Calabria highway. The bridge was built in the 1960s and retrofitted in the 1990s. Four types of materials can be identified in the Tenza Bridge: 1) the original concrete used in the 1960s when the bridge was built—this accounts for most of the concrete in the structure; 2) the concrete used to strengthen the piers and arches; 3) the original lightly ribbed steel used for the reinforcement of the original concrete; and 4) the new ribbed steel used as reinforcement of the more recent RC portions.

In the first phase of the project, the structure was characterized through static analysis under gravity and live loads and a complete seismic assessment. The finite element method (FEM) model used to perform these analyses was validated by comparing the numerical vibration modes with the results of a vibrodyne test. During such test, an evaluation of the vibration modes was performed processing the acceleration fields acquired using accelerometers distributed on the structure.[1]

The objective of the second phase of the project was to perform an assessment of the structure under severe dynamic loads, such as impact or blast, through numerical analysis and in-place tests. For this purpose, a dynamic characterization of both concrete and steel of the Tenza Bridge, subjected to severe dynamic load conditions, was performed; the results of the activity conducted on concrete represents the specific object of the current article.

In particular, high-strain-rate tensile failure tests were conducted at the DynaMat Laboratory of the University of Applied Sciences of Southern Switzerland, and stress-strain relationships were then evaluated. The strain rate range of interest for concrete was identified between 1 s^{-1} and 50 s^{-1} because these values are related to impact and blast load conditions.[2] The obtained results, widely discussed in the following paragraphs, are fundamental to define the influence of dynamic loads on the constitutive behavior of materials aged in a real structure and provide a reliable point of reference to be used in structural analyses accounting for strain rate effects. Indeed, knowledge of the dynamic behavior of both structure and materials is essential to perform a complete assessment of the bridge under impact or blast loads.

In particular, under such load conditions, two different types of failure can be distinguished[3]: 1) local failure; and 2) global failure.

The former can be due to an impact or an explosion occurring close to structural elements; the characteristics of this failure depend on the dynamic properties and ductility of the element concerned and its constituent materials. By contrast, global failure occurs after local failure and it is related to the ability of the structure to withstand the loss of elements without activating progressive collapse. It depends on global ductility properties of the structure and on the quality and frequency of connections between its elements. Obviously, the more severe the local failure, the more likely global failure is to occur.

Local failure can be distinguished into local failure of materials and local failure of structural elements. The first type of failure occurs when the explosion is so close to the structure that the consequent shockwave in the air, impacting on the surface of the element, causes a high field of compression and propagates a tensile wave inside the material. Hence, these stresses can cause the concrete to crack and, consequently, a projection of debris. By contrast, the second type can occur when the failure of one or more sections within the element is activated.[4]

Instead, global failure takes place after severe damage to one or more structural elements, which can lead to progressive

ACI Structural Journal, V. 106, No. 1, January-February 2009.
MS No. S-2007-252.R2 received January 4, 2008, and reviewed under Institute publication policies. Pertinent discussion including author's closure, if any, will be published in the November-December 2009 *ACI Structural Journal* if the discussion is received by July 1, 2009.

Domenico Asprone *is a PhD Student at the University of Naples Federico II, Naples, Italy, where he received his MS in civil engineering. His research interests include the behavior of structures under high dynamic loads and the related retrofitting techniques.*

Ezio Cadoni *is a Professor at the University of Applied Sciences of Southern Switzerland, Lugano, Switzerland. He received his MS in civil engineering from the University of Cagliari, Cagliari, Italy, and his PhD from the Polytechnic University of Turin, Turin, Italy. His research interests include impact and dynamic behavior of materials and structures, durability, and nondestructive techniques.*

ACI member **Andrea Prota** *is an Assistant Professor of structural engineering at the University of Naples Federico II. He received his Master of Science in civil engineering from the University of Missouri-Rolla, Rolla, MO, and his PhD in structural engineering at the University of Naples Federico II. He is a member of ACI Committee 440, Fiber Reinforced Polymer Reinforcement. His research interests include behavior of reinforced concrete and masonry structures under man-made and natural extreme loads, the use of advanced materials for new construction, and the retrofit of existing structures using innovative techniques.*

collapse of the structure. Hence, the possibility of this failure mechanism is linked to the capacity of the structure to redistribute loads on other structural elements, and it depends on redundancy of the elements and ductility of connections.[5]

Undoubtedly, in the case of the bridge, the piers and the arch are fundamental to guarantee the equilibrium of the entire structure. The arch, with its massive section, has a very low probability of failure under a blast event, albeit particularly severe. Therefore, progressive collapse analyses focus on the loss of the piers. Obviously, this consideration also influences local failure analyses, which are more detailed for the piers.

As explained previously, the current research focuses the attention on the dynamic characterization of concrete of the Tenza Bridge, which represents a fundamental phase in the blast assessment process, performed in the Tenza project.

RESEARCH SIGNIFICANCE

Various experimental campaigns have been carried out on the tensile dynamic behavior of concrete in recent decades,[6] but very few investigations have been performed on existing concrete taken from a real structure, mainly examining low strain rate ranges induced by seismic loading conditions.[7] Hence, the main significance of the current research is evaluation of the tensile dynamic properties of an existing concrete under high strain rates, to confirm that the exhibited behavior would be as expected, according to available literature. Comparisons were thus performed between the obtained strength data and the existing tensile strength dynamic increase factor (DIF)-strain rate formulations, where DIF is defined as the ratio of the dynamic value of a mechanical parameter over its corresponding static value. The results confirmed that the available relationships provide good predictions of the mechanical behavior of concrete under dynamic loads, even if it is taken from an existing structure.

DESCRIPTION OF STRUCTURE

Tenza Bridge

The Tenza Bridge (Fig. 1) was open to traffic until a few years ago. Indeed, recently, ANAS, the Italian road agency that owns the bridge, planned to change the geometry of the route because the current route no longer conforms to current safety standards. Therefore, the bridge was closed to traffic as it belonged to a replaced section of the highway.

The bridge structure of the Tenza viaduct consists of three different structures: a central superior way arch bridge and two approach viaducts. The arch structure is 120 m (393.7 ft) long and 40 m (131.2 ft) deep, while each arch approach ramp is approximately 30 m (98.4 ft) long.

Fig. 1—View of Tenza Bridge.

The bridge deck consists of a ribbed slab and is supported by multiple RC columns of different heights, linking the slab to the arch. Each individual support is made of two columns that, apart in the central zone of the bridge, are connected over their entire height by an RC wall. In the 1990s, the structure was strengthened by RC jacketing of the columns and widening the arch section.

Traditional assessment and characterization

The aim of the first phase of the project was to obtain detailed knowledge of bridge properties and structural behavior prior to a traditional investigation. First, the actual bridge geometry was evaluated by analyzing the original drawings and acquiring data with a three-dimensional laser scanner survey; a static characterization of materials was then conducted. After this phase, an FEM model was built. Subsequently, modal analysis was performed and validated through a vibrodyne in-place test to ensure the reliability of the FEM model. Finally, static analysis under gravity and seismic loads was conducted to perform a traditional assessment of the bridge. Detailed results of this phase may be found in Reference 1.

STATIC CHARACTERIZATION OF CONCRETE

The aim of this test campaign was to obtain a complete quasistatic characterization of the concrete of the Tenza Bridge. As already explained, two types of concrete can be identified in the structure: the concrete used in the 1960s (when the bridge was built), and the concrete used for piers and arch strengthening. For both types, several specimens were taken from the real structure and compression tests were performed. Unfortunately, there was no information from original construction documents about concrete strength, cement type, size of coarse aggregate, water/cement ratio (w/c), admixtures used, or results of quality assurance tests for both types of concrete.

Concrete cores were collected to achieve a representative characterization of the entire structure and then account for the spatial homogeneity of mechanical properties of concrete. With this aim, specimens were taken from the arch and piers in regions close to the base and midspan of the bridge, and from the upper deck, at three different points of the wheel path. The specimens were cylinders with a diameter of either 75 or 100 mm (2.95 or 3.94 in.) and variable lengths. Compression test data were processed using the following European Standard relationship[8]

$$R_{cub} = \frac{R_{measured} \times D}{1.5 + \left(\frac{1}{\lambda}\right)} \quad (1)$$

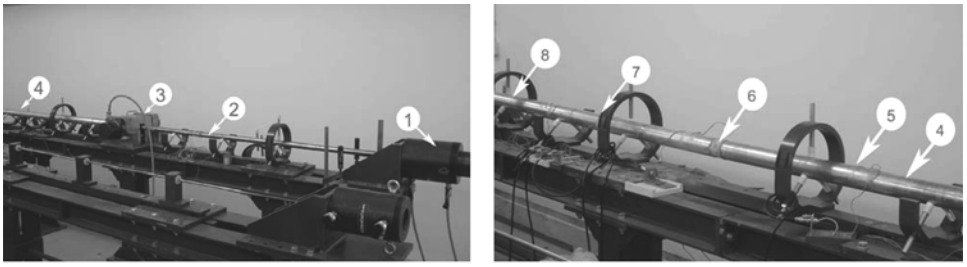

1. hydraulic actuator; 2. high-strength steel bar for energy storage (3m); 3. blocking device; 4. input bar; 5. strain gauges to measure incident and reflected pulses; 6. specimen; 7. strain gauges to measure transmitted pulses; and 8. output bar.

Fig. 2—Experimental setup.

Table 1—Static compression test results

Extraction zone of specimens	Average cubic strength, MPa (psi)	Average cylindrical strength, MPa (psi)
Deck (original concrete)	55.89 (8106)	46.39 (6728)
Arch (original concrete)	41.10 (5961)	34.11 (4947)
Arch (strengthening concrete)	37.51 (5440)	31.13 (4515)
Piers (original concrete)	40.08 (5813)	33.27 (4825)
Piers (strengthening concrete)	36.55 (5301)	30.33 (4399)

where R_{cub} is the compressive cubic strength; D = 2.3 for vertical extraction and D = 2.5 for horizontal extraction; and λ is the height/diameter. Multiplying the cubic strength by a coefficient of 0.83, the value of the cylindrical strength was then calculated.[9]

The processed data (Table 1) show that the original concrete, especially in the deck, has a higher average compressive cylindrical strength compared with that of the strengthening concrete. This is probably due to the long curing period (approximately 40 years) of the old concrete.

DYNAMIC TESTS ON CONCRETE

Introduction to dynamic properties of concrete

The differences between dynamic and static properties of concrete are amply illustrated in the literature.[2,6,7,10-15] It is accepted that, to correctly evaluate the behavior of concrete under extreme dynamic loads, dynamic mechanical properties have to be necessarily investigated. The scientific data available show that, under high strain rates, concrete can exhibit, under both compression and tensile loads: 1) an increase in failure strength[6-10]; 2) an increase in Young's modulus[6,11,16,17]; and 3) a different evolution of cracks that do not develop through a local mechanism, like in a static range, but start and grow at the same time in several locations.[11] Moreover, an increase in strength is exhibited, both in compression and in tension, for flexural loads.[10,18]

These characteristics are explained by several technical codes or instructions to guide the engineer to properly predict the real behavior of a structure under extreme loads. *CEB Information Bulletin* No. 187[2] gives formulations to evaluate the dynamic properties of concrete by updating static properties. DIF-strain rate relationships are suggested for compressive and tensile failure stresses, compressive and tensile ultimate strains, and Young's modulus. TM 5-1300[4] is a technical document that gives specific guidelines for structures subjected to blast loads. It has a very direct approach to structural design and gives detailed indications for several design situations of different structures under explosions. The issue of the dynamic properties of concrete is considered by suggesting different DIF for failure strength in several load conditions. In this case, the DIF is not a function of strain rate value, as expressed by CEB formulations, but it just depends on the distance from the blast source, distinguishing between far away and in-close explosions.

DynaMat facilities

To determine the mechanical properties of concrete under high loading rates, a dynamic test campaign was conducted at the DynaMat Laboratory of the University of Applied Sciences of Southern Switzerland (SUPSI) of Lugano. The laboratory is equipped with four modified Hopkinson bar (MHB)[19] apparatuses 15 m (16.4 yd) in length with diameters of 60 mm (2.36 in.) for concretes and rocks; 10 and 12 mm (0.39 and 0.47 in.) for metals, ceramics, and glass; and 20 mm (0.79 in) for polymers, fiber-reinforced polymers, and mortars; a hydro-pneumatic machine (HPM); and two universal machines for quasistatic tests. The MHB and the HPM allow carrying out tensile failure tests with a strain rate ranging from 1 s^{-1} to 10,000 s^{-1} and from 0.1 s^{-1} to 50 s^{-1}, respectively.

Setup for high-strain-rate tests

The tests were performed using the MHB system. Concrete specimens were cylindrical, with both diameter and height of 60 mm (2.36 in.). The system used to perform the tests consisted of two circular aluminum bars, with a length of 3 m (9.84 ft) and a diameter of 60 mm (2.36 in.). The specimens were positioned between the two bars and glued to them using an epoxy resin (refer to Fig. 2 and 3). During the test, each bar was equipped with semiconductor strain gauges to obtain measurements of the incident, and reflected and transmitted pulses acting on the cross section of the specimens during the test. The concrete specimen was also instrumented with a strain gauge.

The phases of a tensile failure test performed using an MHB machine can then be summarized as follows:

- A hydraulic actuator, of maximum loading capacity of 1 MN, pulls a high-strength steel bar with a length of 3 m (9.84 ft) and a diameter of 35.8 mm (1.41 in.); the pretension stored in this bar is resisted by the blocking device (Fig. 2) linked to the first of the aluminum bars, called the input bar; and
- The fragile bolt in the blocking device then fails, giving rise to a tensile mechanical pulse duration of 1200 μs, with a linear loading rate during the rise time, propagating along the input bar and then transmitted, through the concrete specimen, to the second aluminum bar, called the output bar. Then pulses acting on the specimen determine its failure (Fig. 4).

Aluminum was chosen as the bar material because of its acoustic impedance, which is not far from that of plain concrete. In fact, the longitudinal acoustic impedance is

approximately 19,500 and 38,000 kg/s (42,990 and 83,775 lb/s) for concrete specimens and aluminum bars, respectively. This minimizes the constraint to transverse deformation of the concrete specimen that depends on the ratio between the Poisson's ratio and Young's modulus. The strain gauge station on the input bar measures the incident pulses ε_I and the reflected pulses ε_R. The strain gauge station on the output bar measures the pulses ε_T transmitted through the specimen.

From the measurement of the reflected and transmitted pulse, the stress and strain history is obtained using the formulation of the Hopkinson theory[20]

$$\sigma(t) = E_0 \frac{A_0}{A} \varepsilon_T(t) \tag{2}$$

$$\varepsilon(t) = -\frac{2C_0}{L} \int_0^t \varepsilon_R(t)dt \tag{3}$$

$$\dot{\varepsilon}(t) = -\frac{2C_0}{L} \varepsilon_R(t) \tag{4}$$

where $\sigma(t)$ represents the longitudinal stress in the specimen; $\varepsilon(t)$ represents the longitudinal strain in the specimen; $\varepsilon_T(t)$ represents the longitudinal strain transmitted in the output bar; $\varepsilon_R(t)$ represents the longitudinal strain reflected in the input bar; $\dot{\varepsilon}(t)$ represents the strain rate in the specimen; E_0 is the elastic modulus of the bars; A_0 is their cross-sectional area; A is the specimen cross-sectional area; L is the specimen length; and C_0 is the sound velocity of the bar material.

The test data were acquired using a transient recorder device, characterized by six fast data acquisition transient recorder channels. The system is designed to provide high-precision (12 bit) waveform acquisition and analysis capabilities with a maximum 50 MS/s real-time sampling rate, 25 MHz full-power bandwidth and acquisition memory of 128K samples per channel. Each individual board has its own independent trigger circuitry and time base, such that one can record with different time windows.

The data acquisition system receives signals from the programmable transducer amplifiers. This is an expandable signal conditioning system that allows the user to configure each individual signal conditioner. Individual channels may be addressed, or an all-channel command will address all channels simultaneously for fast initial setup. Figure 5 presents the logical architecture of the experimental measurements and recordings.

During the experimental campaign, the specimens were divided into four categories: 1) the original arch concrete; 2) the arch strengthening concrete; 3) the pier original concrete; and 4) the pier strengthening concrete.

For each concrete, a static tensile test and several dynamic tensile tests were performed. The dynamic tests were conducted focusing on the interesting strain rate values, as defined previously, ranging from soft impact values (1 s^{-1} to 10 s^{-1}) to hard impact values (10 s^{-1} to 50 s^{-1}). Unfortunately, no dynamic tests were conducted on deck concrete due to unavailability of cores. For the dynamic assessment of the structure, however, it is conservative to assume that dynamic properties of deck concrete are similar to those of the concrete from the arch and the piers because, under quasistatic conditions, it revealed even higher resistances.

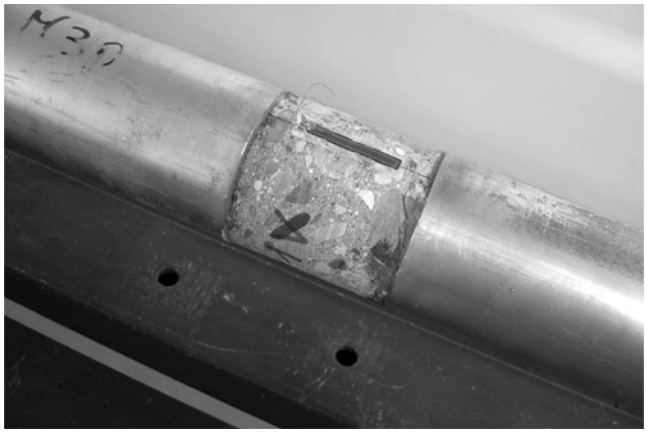

Fig. 3—Concrete specimen in Hopkinson bar.

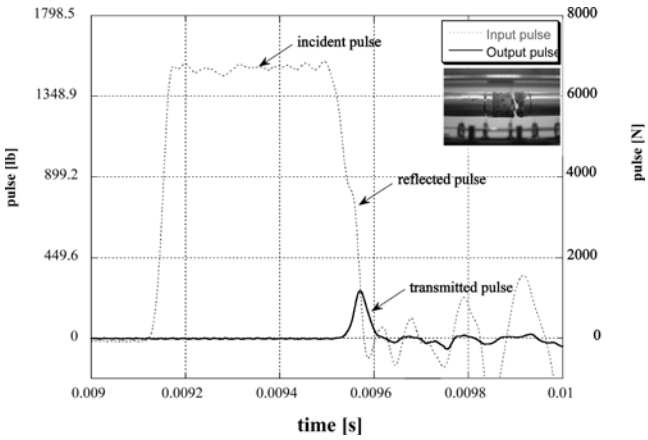

Fig. 4—Acquired signal measurement by input and output bar strain-gauge stations.

Test results

Direct data acquisition is represented by two strain-time curves provided by strain gauge sensors positioned on input and output bars. Multiplying strain values by the elastic modulus of bars, they can be related to pulses moving through the system, which is composed by the input bar, the specimen, and the output bar. Figure 4 shows an example of the transformation of acquired data into forces acting on the system.

Moreover, using strain-time curves read by sensors on input and output bars, through Eq. (2) and (3), stress-time and strain-time curves can be evaluated for concrete specimens. Then, using time as a common parameter of the two last curves, stress-strain relationships can be processed for the specimen at the strain rate given by Eq. (4). The average values of the obtained results in terms of failure stress, ultimate strain, and fracture energy are presented in Table 2.

Importantly, during such tests, the strain rate has no constant value. Hence, definition of the strain rate value for each test is not straightforward. Frequently in the literature, the maximum value of strain rate is chosen as the strain rate level. In this study, a different approach was preferred, defining the strain rate level as the strain rate obtained at the time when there was maximum stress.

An example of stress-strain curves is shown in Fig. 6, and Fig. 7 depicts different results in terms of stress-time curves for the same strain rate and the same concrete type; it can be noticed that result dispersion for such tests is not different from that appreciable in static failure tests. Figure 8 shows a

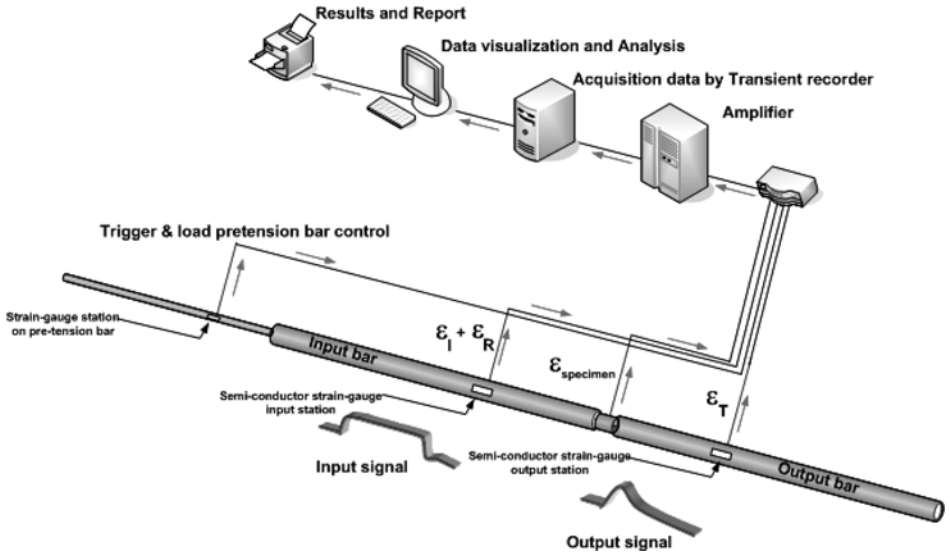

Fig. 5—Logical architecture of experimental measurements.

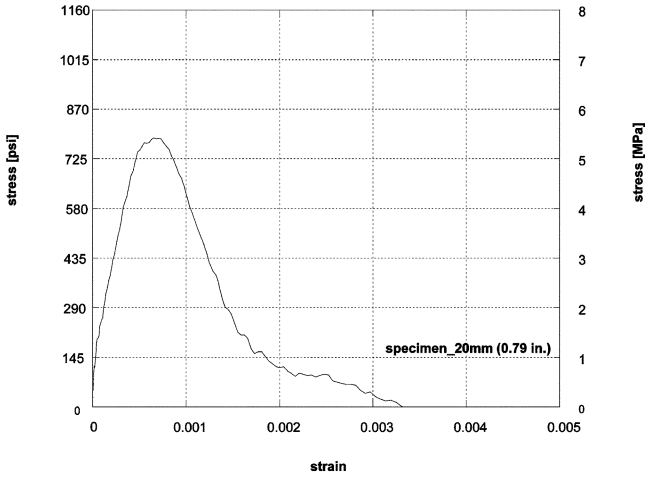

Piers new concrete specimen tested at a strain rate of 52 s^{-1}: fracture strain: ε_u=654 με; fracture stress: f_{ct}=5.43 MPa (787.6 psi)

Fig. 6—Example of tensile stress versus strain acquisition.

concrete specimen after its failure. As it is typically observed in these types of experiments, a single crack develops approximately in the middle of the specimen length, induced by uniform tensile stresses acting along the specimen cross section.

The main results are shown in Fig. 9. They represent the main tensile stress-strain curves of arch and pier concrete at different strain rates. It can be observed from Table 2 that tensile strength and total deformation energy (evaluated as the area under the curves) increase as the strain rate increases. Interestingly, for the concrete of original portions, even though the specimens were taken from a 46-year-old existing structure, the observed trend is consistent with the results described in the literature.[2,10-15]

ASSESSMENT OF EXPERIMENTAL RESULTS

To correctly analyze the influence of the strain rate on the mechanical properties of concrete, the results in terms of failure strength were elaborated to obtain the DIF, thereby obtaining the curves in Fig. 10. Moreover, to verify that the obtained data were consistent with results described in the literature, a comparison with existing theories was performed. As points of reference, the CEB[2] and Malvar and Ross[12]

Table 2—Results of dynamic tensile tests

Extraction zone of specimens	Strain rate	$d\varepsilon/dt$, s^{-1}	f_{ct}, MPa (psi)	ε_u, με	Fracture energy, J/m^2 (lb-in./$in.^2$)
Arch (original concrete)	Quasi-static	10^{-4}	2.89 (419)	120	—
	Soft impact	1	3.54 (513)	444	360 (2.06)
	Hard impact	10	4.84 (702)	458	238 (1.36)
Arch (strengthening concrete)	Quasi-static	10^{-4}	3.40 (493)	160	—
	Hard impact	10	6.73 (976)	587	373 (2.13)
Piers (original concrete)	Quasi-static	10^{-4}	1.87 (271)	—	—
	Soft impact	1	2.38 (345)	644	137 (0.78)
	Hard impact	10	4.54 (658)	538	262 (1.50)
Piers (strengthening concrete)*	Quasi-static	10^{-4}	2.91 (422)	—	—
	Soft impact	5	5.87 (851)	1090	—
	Hard impact	50	5.94 (862)	736	135 (0.77)
	Hard impact	70	11.67 (1693)	862	148 (0.85)

*Tests were carried out on small specimens; h/d = 1; d = 20 mm (0.79 in.).
Notes: f_{ct} is fracture stress and ε_u is ultimate strain.

expressions were considered. Both of these formulations seek to predict dynamic tensile strength, expressing the DIF as a function of the strain rate; the CEB formulation expresses the DIF as

$$\text{DIF} = \frac{f_d}{f_s} = \left(\frac{\dot{\varepsilon}}{\dot{\varepsilon}_0}\right)^{1.016\delta} \quad \text{for} \quad \dot{\varepsilon} \le 30 \text{ s}^{-1} \tag{5}$$

$$\text{DIF} = \frac{f_d}{f_s} = \eta\left(\frac{\dot{\varepsilon}}{\dot{\varepsilon}_0}\right)^{\frac{1}{3}} \quad \text{for} \quad \dot{\varepsilon} > 30 \text{ s}^{-1} \tag{6}$$

where f_d is the dynamic strength; f_s is the static strength; $\dot{\varepsilon}$ is the strain rate; $\dot{\varepsilon}_0$ is a constant equal to 3×10^{-6} s^{-1} and has the meaning of the static strain rate; $\log\eta = 7.11\delta - 2.33$, where

$$\delta = \frac{1}{10 + 6\dfrac{f_{cs}}{f_0}};$$

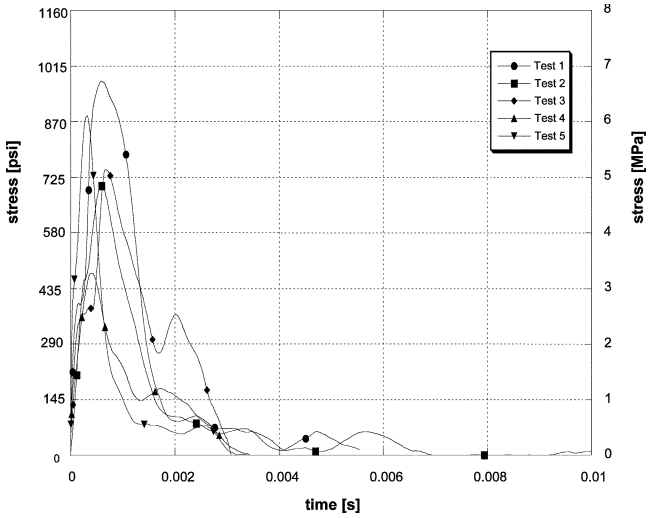

Fig. 7—Comparison between stress-time curves for concrete specimens of same extraction zone at same strain rate (10 s^{-1}).

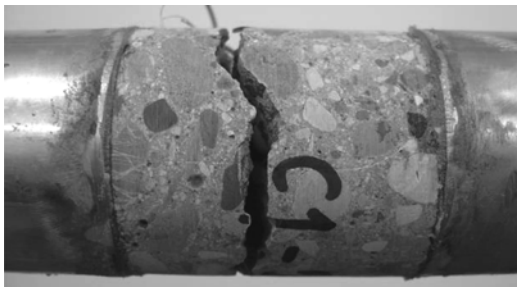

Fig. 8—Concrete specimen after failure.

f_{cs} is the static compressions strength; and f_0 is constant equal to 10 MPa (1450 psi).

This formulation gives the DIF as a bilinear function of the strain rate in the logarithmic scale, and presents a slope variation at 30 s^{-1}. The following Malvar formulation, instead, expresses the DIF in a similar way but fixes the reference static strain rate at 10^{-6} s^{-1} and moves the slope variation to 1 s^{-1}

$$\text{DIF} = \frac{f_d}{f_s} = \left(\frac{\dot{\varepsilon}}{\dot{\varepsilon}_{0M}}\right)^{\delta_M} \quad \text{for} \quad \dot{\varepsilon} \le 1 \text{ s}^{-1} \tag{7}$$

$$\text{DIF} = \frac{f_d}{f_s} = \beta\left(\frac{\dot{\varepsilon}}{\dot{\varepsilon}_{0M}}\right)^{\frac{1}{3}} \quad \text{for} \quad \dot{\varepsilon} > 1 \text{ s}^{-1} \tag{8}$$

where f_d, f_s, and $\dot{\varepsilon}$ have already been expressed previously; $\dot{\varepsilon}_{0M}$ is a constant equal to 10^{-6} s^{-1}; $\log\beta = 6\delta_M - 2$, where

$$\delta_M = \frac{1}{1 + 8\frac{f_{cs}}{f_0}};$$

and f_{cs} and f_0 have already been defined previously.

By plotting these relationships against the experimental results (Fig. 10), the correspondence with the data obtained can then be appreciated. Moreover, Table 3 reports the DIFs

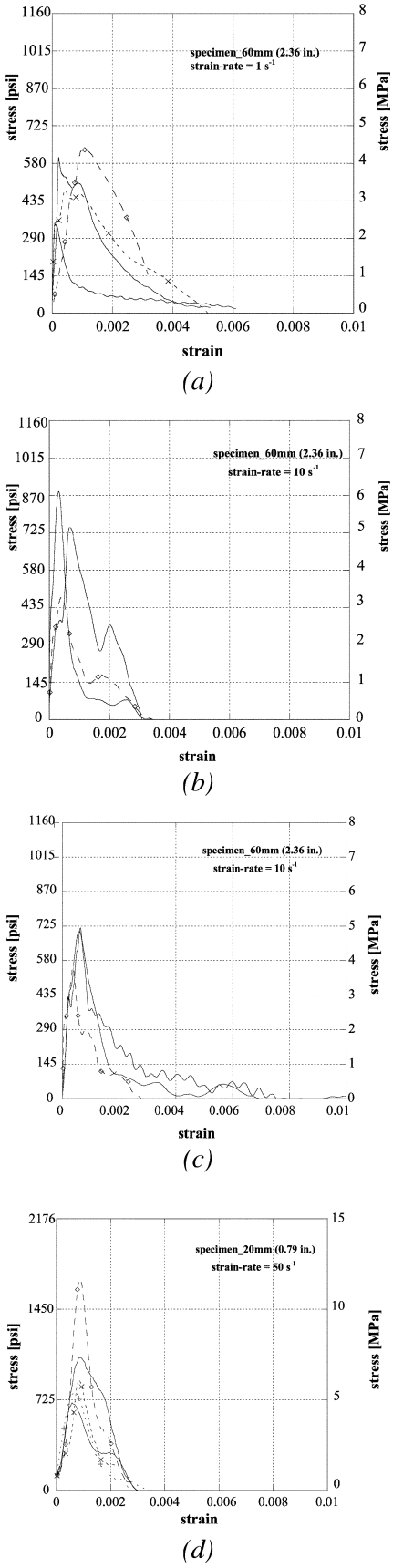

Fig. 9—Stress-strain curves of: arch original concrete at a strain rate of (a) 1 s^{-1} and (b) 10 s^{-1}; (c) stress-strain curves of pier original concrete at strain rate of 10 s^{-1}; and (d) stress-strain curves of pier strengthening concrete at strain rate of 50 s^{-1}.

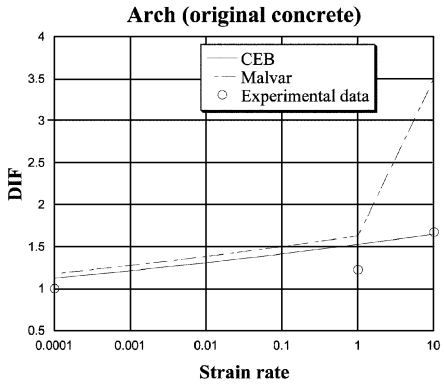

(a)

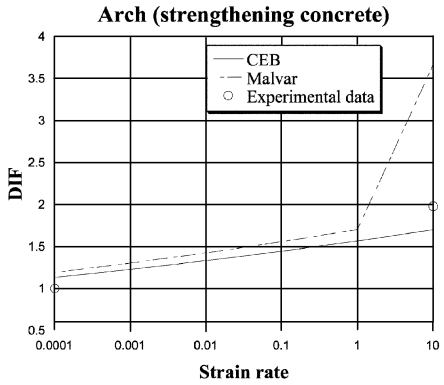

(b)

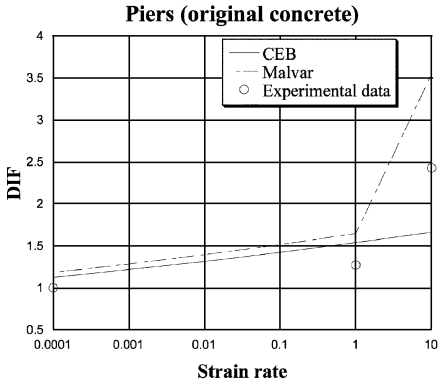

(c)

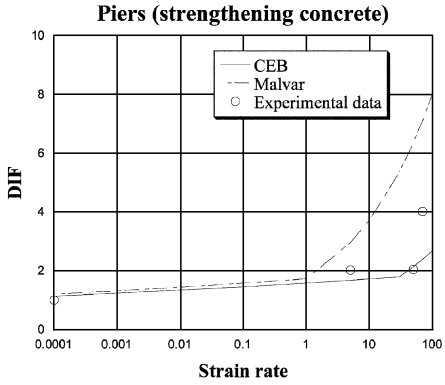

(d)

Fig. 10—Failure stress DIF for: (a) arch original concrete; (b) arch strengthening concrete; (c) pier original concrete; and (d) pier strengthening concrete.

Table 3—Experimental and numerical DIF of tensile strength

Extraction zone of specimens	Strain rate	$d\varepsilon/dt$, s^{-1}	DIF of tensile strength		
			Experimental values	CEB expression*	Malvar expression*
Arch (original concrete)	Soft impact	1	1.22	1.53 (+25%)	1.63 (+33%)
	Hard impact	10	1.67	1.64 (–1%)	3.51 (+110%)
Arch (strengthening concrete)	Hard impact	10	1.98	1.70 (–14%)	3.67 (+86%)
Piers (original concrete)	Soft impact	1	1.27	1.54 (+21%)	1.64 (+30%)
	Hard impact	10	2.43	1.66 (–31%)	3.55 (+46%)
Piers (strengthening concrete)	Soft impact	5	2.02	1.68 (–17%)	2.95 (+46%)
	Hard impact	50	2.04	2.14 (+5%)	6.37 (+212%)
	Hard impact	70	4.01	2.39 (–40%)	7.12 (+78%)

*Terms in parentheses represent percent differences between numerical and experimental values.

of the tensile strength as evaluated experimentally and numerically through CEB and Malvar expression. Furthermore, the percent differences between numerical and experimental values are presented. This shows that, as Malvar formulation suggests, the slope variation is significant at 1 s^{-1}. In any event, the CEB expression often underestimates or, at the very least, slightly overestimates, the experimental results, whereas the Malvar expression sometimes predicts a higher DIF than the test value. Hence, the CEB expression appears more suitable for designing calculations where more conservative values should be considered.

CONCLUSIONS

In this study, which is part of a wider research project about the Tenza Bridge, the tensile dynamic behavior of the concrete in question was investigated. Several dynamic failure tests were conducted on concrete specimens using a modified Hopkinson bar. Stress-strain relationships were then obtained at different strain rates ranging from 1 s^{-1} to 50 s^{-1}; this range was considered to account for soft and hard impact load conditions. The results were then processed in terms of DIF of the tensile failure strength versus strain rate. Such relationships were finally compared with formulations proposed in the available literature.

The conclusions may be summarized as follows:

1. The performed tests confirmed that the concrete of an old structure is also strain-rate sensitive, as is widely pointed out concerning new concrete;

2. The original concrete is characterized by lower DIF value, if compared with the strengthening concrete; this is probably due to the higher curing level, which makes it dryer and consequently less sensitive to strain rate effect.

3. Both CEB and Malvar DIF-strain rate formulations for tensile strength predict the actual behavior of concrete well;

4. The CEB expression slightly underestimates, whereas the Malvar expression overestimates, the experimental data in many cases. In fact, as can be noticed in Table 3, the maximum obtained percent difference is +40% in the case of the CEB expression and +212% in the case of the Malvar expression. Therefore, the CEB expression appears sounder

for the purpose of design assessment because it provides lower values for the dynamic tensile strength of concrete; and

5. Although both Malvar and CEB expressions give the DIF-strain rate relationship as a bilinear function in logarithmic scale, they consider different positions for the slope variation; based on the tests performed, the variation in gradient occurs at 1 s^{-1}, as predicted by the Malvar formulation.

These results could provide a basic tool for engineers involved in assessing RC structures with respect to extreme loads. Moreover, such data could be useful to build a wider database on dynamic properties of existing concrete, which could be employed to propose useful design relationships, providing mechanical parameters of concrete under different strain rates.

ACKNOWLEDGMENTS

The authors would like to thank the research center Analysis and Monitoring of Environmental Risk (AMRA), which supported the activities presented in the paper. We are also grateful to M. Dotta and the technicians at the University of Applied Sciences of Southern Switzerland and the University Federico II of Naples for carrying out the experiments in dynamic and static fields, respectively.

REFERENCES

1. Asprone, D.; Cosenza, E.; Manfredi, G.; Occhiuzzi, A.; Prota, A.; and Devitofranceschi, A., "Caratterizzazione dinamica di strutture da ponte: il progetto Tenza," *Sperimentazione su Materiali e Strutture*, National Conference Proceedings, Italy, Dec. 2006, pp. 621-631.

2. Comité Euro-International du Béton, "Concrete Structures Under Impact and Impulsive Loading," *CEB Bulletin* No. 187, Lausanne, Switzerland, 1988, 184 pp.

3. Winget, D. G.; Marchand, K. A.; and Williamson, E. B., "Analysis and Design of Critical Bridges Subjected to Blast Loads," *Journal of Structural Engineering*, ASCE, V. 131, No. 8, Aug. 2005, pp. 1243-1255.

4. Departments of the U.S. Army, Navy, and Air Force, "Structures to Resist the Effects of Accidental Explosions (TM 5-1300)," Nov. 1990, 1796 pp.

5. NIST/GSA, "Workshop on Application of Seismic Rehabilitation Technologies to Mitigate Blast-Induced Progressive Collapse," Oakland, CA, Sept. 2001, 17 pp.

6. Fu, H. C.; Erki, M. A.; and Seckin, M., "Review of Effects of Loading Rate on Concrete in Compression," *Journal of Structural Engineering*, V. 117, 1991, pp. 3645-3659.

7. Harris, D. W.; Mohorovic, C. E.; and Dolen, T. P., "Dynamic Properties of Mass Concrete Obtained from Dam Cores," *ACI Materials Journal*, V. 97, No. 3, May-June 2000, pp. 290-296.

8. EN 12504-1,"Testing Concrete, Part 120—Methods for Determination of the Compressive Strength of Concrete Cores," British Standard 1881, 2000, 12 pp.

9. EN 1992-1-1:2004, "Eurocode 2: Design of Concrete Structures. General Rules and Rules for Buildings," 2004, 230 pp.

10. Cadoni, E.; Solomos, G.; Berra, M.; and Albertini, C., "High Strain-Rate Behaviour of Plain Concrete Subjected to Tensile and Compressive Loading," *Proceedings of the Third International Conference on Construction Materials: Performances, Innovations, and Structural Implication*, Paper no. 1.12.6., Vancouver, BC, Canada, Aug. 2005. (CD-ROM)

11. Cadoni, E.; Labibes, K.; Berra, M.; Giangrasso, M.; and Albertini, C., "High Strain-Rate Tensile Behaviour of Concrete," *Magazine of Concrete Research*, V. 52, No. 5, Oct. 2000, pp. 365-370.

12. Malvar, L. J., and Ross, C. A., "Review of Strain-Rate Effects for Concrete in Tension," *ACI Materials Journal*, V. 95, No. 6, Nov.-Dec. 1998, pp. 735-739.

13. Cadoni, E.; Albertini, C.; Labibes, K.; and Solomos, G., "Behavior of Plain Concrete Subjected to Tensile Loading at High Strain-Rate," *Proceeding of the Fourth International Conference on Fracture Mechanics of Concrete and Concrete Structures (FRAMCOS-4)*, Cachan, France, 2001, pp. 341-348.

14. Cadoni, E.; Albertini, C.; and Solomos, G., "Analysis of the Concrete Behavior in Tension at High Strain-Rate by a Modified Hopkinson Bar in Support of Impact-Resistant Structural Design," *Journal de Physique*, V. 3, 2006, pp. 647-652.

15. Albertini, C.; Cadoni, E.; and Labibes, K., "Mechanical Characterization and Fracture Process of Concrete at High Strain Rates," *Proceedings of the Second International Conference on Concrete under Severe Conditions (CONSEC '98)*, Tromsø, Norway, 1998, pp. 735-744.

16. Toutlemonde, F.; Boulay, C.; and Rossi, P., "High Strain-Rate Tensile Behaviour of Concrete: Significant Parameters," *Proceedings of the Second International Conference on Fracture Mechanics of Concrete and Concrete Structures (FRAMCOS-2)*, Freiburg, Germany, 2005, pp. 709-718.

17. van Doormal, J. C. A. M.; Weerheijn, J.; and Sluys, L. J., "Experimental and Numerical Determination of the Dynamic Fracture Energy of Concrete," *Journal de Physique*, V. 4, 1994, pp. 501-506.

18. Banthia, N.; Mindess, S.; Bentur, A.; and Pigeon, M., "Impact Testing of Concrete Using a Drop-Weight Impact Machine," *Experimental Mechanics*, V. 29, 1989, pp. 63-69.

19. Cadoni, E.; Amaro, W.; Dotta, M.; Albertini, C.; and Giorgetti, P., "DynaMat: Laboratory for Mechanical Characterization of Materials at High Strain-Rate," *Structural Concrete in Switzerland*, FIB-CH, 2006, pp. 35-38.

20. Lindholm, U. S., "High Strain-Rate Tests, in Measurement of Mechanical Properties," *Techniques of Metals Research*, V. 5, 1971, pp. 199-271.